PAPER • OPEN ACCESS

Theoretical study of the low-energy electron-collision cross sections of isomers HOOCl, HOClO and HClOO in gas phase

View the article online for updates and enhancements.

IOP ebooks™

Bringing you innovative digital publishing with leading voices to create your essential collection of books in STEM research.

Start exploring the collection - download the first chapter of every title for free.

Theoretical study of the low-energy electron-collision cross sections of isomers HOOCl, HOClO and HClOO in gas phase

Milton M Fujimoto[1], Mylena H Ribas[1], Jhenifer M Hummel[1], Gabriel L C de Souza[2] and Jonathan Tennyson[3,4]

[1] Departamento de Física, Universidade Federal do Paraná, 81531-990 Curitiba, PR, Brazil
[2] Departamento de Química, Universidade Federal de Mato Grosso, 78060-900 Cuiabá, MT, Brazil
[3] Department of Physics & Astronomy, University College London, Gower St., London, WC1E 6BT, United Kingdom

E-mail: milton@fisica.ufpr.br and j.tennyson@ucl.ac.uk

Abstract

Cross sections for the elastic electron scattering by HOOCl, HOClO and HClOO isomers are calculated using the *R*-matrix method. A systematic study considering basis set, polarisation and the Born closure technique is performed. Low-energy resonances are found for both HOOCl and HOClO, near 1.7 and 1.2 eV respectively, but not for HClOO. The lowest-energy resonance for HClOO is observed at 4.5 eV. Basis sets and polarisation effects on the differential cross sections are found to be important for scattering energies below 5 eV for HOOCl and HOClO due to the presence of these resonances. The dependence of the molecular dipole moment on target basis set used affects the integral cross sections (ICS) results. The ICS for HOClO is larger than other two isomers due to its larger dipole moment, around 3.2 D, while the ICS for HOOCl and HClOO have similar magnitude as both their dipole moments are near 1.9 D. Estimated dissociative electron attachment (DEA) cross sections suggest that HOOCl and HOClO will undergo DEA with low-energy electrons but that HClOO requires higher-energy electrons to undergo DEA.

Supplementary material for this article is available online

Keywords: elastic collisions, isomers, dissociative electron attachment, *R*-matrix, different cross sections, chlorous acid

(Some figures may appear in colour only in the online journal)
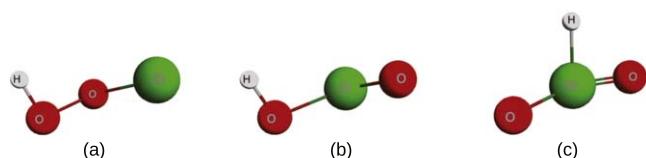
1. Introduction

Understanding the role played by atmospheric pollutants in the Earth's atmosphere is important for tackling large scale problems such as climate change and ozone layer depletion. Molina and Rowland (1974) showed that ozone molecules

[4] Author to whom any correspondence should be addressed.

could be destroyed catalytically by chlorine atoms produced by ultra-violet (UV) irradiation of chlorofluorocarbons (CFCs) molecules and suggested that stable halogenated aliphatic hydrocarbons could be chlorine atoms reservoir which were added to the atmosphere in large quantities. The net destructive of O_3 was schematically represented by catalytic chain reactions

$$Cl + O_3 \rightarrow ClO + O_2, \tag{1}$$

$$ClO + O \rightarrow Cl + O_2 \tag{2}$$
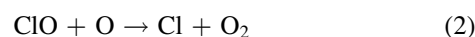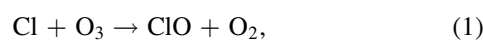
which could occur in the Earth's atmospheric ozone layer in stratosphere. This work was followed by many theoretical and experimental studies of the details of reactions aimed at

Figure 1. Structure of the isomers (a) HOOCl, (b) HOClO and (c) HClOO. (Figure generated with help of MacMolplt software (Bode and Gordon 1998).)

understanding the mechanism of ozone depletion and to propose models which predict the ozone concentrations or destruction; for an overview of these studies see the interesting reviews by Smith (2003) and Cox (2003) and the compilation by the US National Research Council (1989).

In 1985, Farman *et al* (1985) reported an 'ozone hole' over Antarctica during spring time when large depletion of ozone was observed in the stratosphere. The ozone layer was being destroyed faster than any model predicted. This caught the attention of global scientific community and kick started intensive research into atmospheric chemistry with the aim of improving knowledge about the complex mechanism of ozone depletion in the upper atmosphere. Many mechanisms for ozone depletion were proposed with halogenated molecules, such as CFCs, playing a central role in producing reactive halogen atoms or halogenated molecules. There are many mechanisms for ozone destruction which rely on chlorine atoms and reaction intermediate chlorine-containing molecules. The reactions of numerous intermediate species have been studied theoretically or experimentally, such as those of ClO (Molina and Rowland 1974, Cox 2003) and its dimer (Molina and Molina 1987, Barrett *et al* 1988), $H_xCl_yO_z$ (McGrath *et al* 1990, Phillips and Quelch 1996, Dubey *et al* 1998), and Cl_xO_yN (Colussi and Grela 1993).

An interesting reaction intermediary proposed in many chain reactions involving chlorine atoms is chlorous acid, HOClO. This specie has 2 other isomers: HOOCl and HClOO. The figure 1 presents the chemical structures of these three isomers, which we will refer to collectively as $HClO_2$ below. Weissman *et al* (1981) proposed HOOCl as a reaction intermediate which appears in the reaction $HO_2 + Cl \rightleftharpoons [HOOCl]^* \rightleftharpoons HCl + O_2$ and estimated its atmospheric lifetime. Many subsequent studies have suggested that HOOCl or its isomers are important reaction intermediary which decay into different products such as HO + OCl (Lee and Howard 1982, Cattell and Cox 1986).

McGrath *et al* (1990) reported a theoretical study of isomers of Cl_2O_2 in which they optimised the equilibrium geometry for HOClO at second-order Møller–Plesset perturbation theory (MP2)/6–31G* level of calculation and also presented normal mode vibrational frequencies, infrared intensities, and its dipole moment. Turner and Oleksik (1991) calculated spectroscopic properties for the two isomers HOOCl and HOClO at Hartree–Fock (HF) and post HF levels. Their results indicated that HOOCl is more stable than its HOClO isomer. Theoretical calculations which determined the geometry, dipole moment, spectroscopic parameters and heat of formation was performed by Lee and Rendell (1993) at the coupled-cluster with Single and Double and

Perturbative Triple excitations (CCSD(T)) level where they verified the stability of HOOCl. Colussi and Grela (1993) used a valence bond additivity scheme and settled thermochemical data to predict heats of formation of various species Cl_xO_yN and HCl_xO_yN. They proposed a complex chain reactions to explain the decomposition of perchloric acid ($HOClO_3$) whereby HOClO is one of the reaction intermediates with a reaction step given by HOClO → HO + ClO. An *ab initio* study at the MP2 and CCSD(T) levels was performed by Francisco *et al* (1994) to determine geometries, relative stability and spectroscopic parameters of the $HClO_2$ isomers. This study found that HOOCl is the more stable with an estimated heat of formation of 1.6 kcal mol^{-1}, followed by HOClO and HClOO which heat of formation are 11.9 and 56.2 kcal mol^{-1}, respectively. They also computed spectroscopic parameters for each isomers which could be used in infrared (IR) spectra to identify them. Phillips and Quelch (1996) investigated some chemical compounds of atmospheric interest involving chlorine atoms, one of them was HOOCl, which they considered as a reaction intermediary in the forward or backward reactions between HO + ClO and HOO + Cl. These authors optimised geometric parameters in multi-configurational self-consistent field (MCSCF) calculations and estimated the enthalpy of reaction for OH + ClO → HOOCl to be -26 kcal mol^{-1} in contrast with -32 kcal mol^{-1} obtained by Weissman *et al* (1981), although still their calculations indicated that the HOOCl specie is stable.

IR spectroscopy was used by Johnsson *et al* (1996) to detect HOClO and HClOO in an argon matrix; the authors compared the calculated band intensities and vibrational frequencies with their observations. Although Francisco *et al* (1994) predicted that HOOCl is the most stable isomer, it was not observed by Johnsson *et al* (1996). Sumathi and Peyerimhoff (1999) performed a scan on the $HClO_2$ potential energy surface (PES) at the MP2 and density functional theory (DFT) levels, and found three minima in the surface. The most thermodynamically stable was HOOCl, followed by HOClO and HClOO in agreement with previous results calculated by Francisco *et al* (1994). Zhu *et al* (2002) studied the kinetics and mechanism of the OH + ClO reaction where both was analysed on both the singlet and triplet PES. This work used DFT method to generate structures of the HOOCl, HOClO, and HClOO reaction intermediaries and their isomerization energy was calculated. The energies of HOClO and HClOO were found to be 7.0 kcal mol^{-1} and 49.2 kcal mol^{-1} above that of HOOCl, respectively, which is consistent with the results of Francisco *et al* (1994). Despite HOOCl being identified as the most stable isomer in various calculations, it was only recently identified by Yoshinobu *et al* (2009). These authors observed HOOCl in neon matrix-isolation IR spectroscopy of an HCl/O_2 mixture when irradiated with vacuum UV light. The assignment of vibrational frequencies to confirm the presence of HOOCl was made with the aid of CCSD(T)/aug-cc-pVDZ calculations.

The interest for low-energy electron-molecule collision has renewed since the pioneering study of Boudaïffa *et al* (2000) which gave evidence that secondary electrons, with energy below 20 eV, interacting with plasmid DNA induced

single and double strand brake in the DNA molecule. Dissociative electron attachment (DEA) is thought to cause the DNA damage mechanism. In this case, a low-energy electron is captured generating a transient anion. If the dissociative potential energy curve of the temporary anion crosses with ground state potential energy curve, there is a probability that it can decay into neutral and negative fragments. Knowledge of resonant states and DEA cross sections provide information about which fragmentation pathways are likely. The HOOCl, HOClO and HClOO isomers are suggested as chlorine reservoirs at the atmosphere and their fragments, according to the authors cited above, participate in intermediary steps in the ozone destruction cycle. DEA of HClO2 isomers could therefore provide a mechanism which produces key intermediate species; such results be important for models of ozone destruction.

In this work we present a theoretical comparative study of gas-phase elastic electron-scattering cross section for the three isomers HOOCl, HOClO and HClOO, calculated using the *R*-matrix method. The study considers the effect of target basis sets, inclusion of polarisation effects and use of the Born closure technique to allow for the long-range effects of the target dipole (Padial *et al* 1981). Of particular importance is the role of low-lying resonances which can lead to breaking of the chemical bonds of the molecule via dissociative electron attachment (DEA). We are unaware of any previous electron collision studies on these molecules. The article is organised as follows: section 2 presents calculation details and the methodology used; section 3 the comparison of results and a discussion are presented. Section 4 presents a summary of main conclusions.

2. Calculation details

2.1. Isomers description

The present work involves an evaluation of how the quality of description of the target affects the cross sections of HOOCl, HOClO and HClOO. The geometry of each isomer was optimised at the CCSD(T)/aug-cc-pVTZ level (de Souza and Brown 2017) and are given in our supplementary data (see table ST.1 is available online at stacks.iop.org/JPB/52/165201/mmedia). All isomers have C_1 symmetry. As the structure of the HOOCl isomer was not known experimentally, it was calculated by Francisco *et al* (1994) who considered three different configurations: cis, trans and skewed. They found that the skewed form has the lowest energy. Our geometry for HOOCl optimized in CCSD(T)/aug-cc-pVTZ level is consistent with the skewed form, as can be seen in the figure 1(a). For electron scattering purposes, we generated the target wave function for the three isomers at the HF level using the following atomic basis sets: TZV (Watchers 1970, Dunning 1971, McLean and Chandler 1980), 6–311G* (Krishnan *et al* 1980, McLean and Chandler 1980) and cc-pVTZ (Dunning 1989). All the basis sets were taken from EMSL Basis Set Library (Feller 1996, Schuchardt *et al* 2007).

The dependence of molecular total energies and dipole moment on these basis sets is presented in table 1 which also gives a comparison with available results in the literature. The relative stability of isomers in our calculation at HF level has the same order as reported by Francisco *et al* (1994), Sumathi and Peyerimhoff (1999) and Zhu *et al* (2002). The HOOCl isomer is the most stable, followed by HOClO and then HClOO for all atomic basis sets calculated.

2.2. R-matrix method

The *R*-matrix method was used to generate low-energy elastic electron-collision cross sections for the gas phase HClO2 isomers. More specifically, the implementation provided by the UK molecular *R*-matrix codes, UKRMol (Carr *et al* 2012), was used in this study. As a description of the UKRMol methodology is given in detail elsewhere (Gillan *et al* 1995, Tennyson 2010), here we only give a brief outline.

In the *R*-matrix method the space is split into two parts: the inner and outer regions. The inner region is delimited by a sphere of radius a, where this radius is chosen to contain the full electronic density of the molecular target, whose centre-of-mass defines the origin of sphere. In the inner region, the exchange, correlation and polarisation interaction are important between continuum electron with the N-electrons of the target. The wave function of $(N + 1)$-electron system in the inner region is represented by

$$\Psi_k^{N+1}(x_1 \ldots x_{N+1}) = \mathcal{A} \sum_{ij} a_{ijk} \phi_i^N(x_1 \ldots x_N) u_{ij}(x_{N+1})$$
$$+ \sum_i b_{ik} \chi_i^{N+1}(x_1 \ldots x_{N+1}), \qquad (3)$$

where $\mathcal{A}$ is an antisymmetrization operator which ensures that the $(N + 1)$-electrons are indistinguishable, ϕ_i^N are the electronic wave functions of the target in the *i*th state and u_{ij} is a one-electron continuum wave function. The polarisation effects on the target wavefunction due to the electric field of the projectile electron can be taken into account by the $(N + 1)$ configurations in the second sum in the right side of equation (3); a_{ijk} and b_{ik} are coefficients determined variationally (Tennyson 1996). To generate the two particle, one-hole (2p,1h) χ_i^{N+1} configurations we have employed up to 50 virtual orbitals taken from the HF calculation including singlet and triplet states in static-exchange-polarisation (SEP) level. The wave function are expanded up to a maximum partial waves $\ell_{\max} = 4$ using GTOs(Gaussian type orbitals) (Faure *et al* 2002).

In the outer region, where the continuum electron is relatively far away, it is not necessary to explicitly consider exchange and correlation effects. In this case, a set of coupled second-order differential equations for the scattering electron functions are solved to calculate scattering observable as a function of electron impact energies. All these isomers possess significant permanent dipole moments and the resulting long-range interaction mean that truncation of partial wave expansion $\ell_{\max} = 4$ is not valid. Higher partial waves are taken into account using a Born closure procedure. The higher partial waves are included in scattering *T*-matrices via analytic Born

Table 1. Molecular properties of HOOCl, HOClO and HClOO isomers with different atomic basis sets.

	This work		Literature	
Basis set	Energy/E_h	Dipole moment/D	Energy/E_h	Dipole moment/D
HOOCl				
TZV	−609.613 444	2.392	−609.667 10[a]	2.00[a]
6–311G*	−609.655 790	2.161	−609.678 66[b]	
cc-pVTZ	−609.701 741	1.885	−610.115 03[c]	
			−610.350 22[d]	1.74[d]
			−610.511 19[e]	
			−611.180 20[f]	
HOClO				
TZV	−609.501 017	3.920	−609.612 02[a]	3.27[a]
6–311G*	−609.601 155	3.579	−610.081 04[c]	2.587[g]
cc-pVTZ	−609.668 433	3.227	−610.497 33[e]	
			−611.165 44[f]	
HClOO				
TZV	−609.051 963	2.179	−609.984 87[c]	
6–311G*	−609.358 707	2.012	−610.428 28[e]	
cc-pVTZ	−609.447 263	1.924	−611.091 25[f]	

[a] From Turner and Oleksik (1991) at HF/6-311G(d,p) level.
[b] From Phillips and Quelch (1996) at Hartree–Fock level.
[c] From Francisco *et al* (1994) at MP2/6-31G(d).
[d] From Lee and Rendell (1993) at CCSD(T)/TZ2P.
[e] From Francisco *et al* (1994) at CCSD(T)/ANO; atomic natural orbital (ANO).
[f] From Sumathi and Peyerimhoff (1999) at B3LYP/6-31G**.
[g] From McGrath *et al* (1990) at MP2/6-31G*.

Table 2. Rotational constants for HOOCl, HOClO and HClOO, in meV.

Isomer	A	B	C
HOOCl	0.201 713 8	0.025 493 4	0.023 049 9
HOClO	0.139 396 1	0.034 416 2	0.028 190 5
HClOO	0.528 911 3	0.036 054 1	0.035 265 7

T-matrices. The rotating dipole approximation is considered to avoid the divergence of fixed-nuclei approximation (Padial *et al* 1981, Morrison 1988). The cross sections are obtained using the code POLYDCS (Sanna and Gianturco 1998) where the rotational excitation cross sections ($J = 0 \rightarrow J' = 0, 1, 2,...$) are summed to convergence which allows us to predict the rotationally-unresolved cross sections which are usually measured. Table 2 presents the molecular rotational constants used for each isomer computed at the equilibrium geometries.

3. Results and discussion

In this section we present a systematic study which gives eigenphase sums, elastic differential cross sections (DCS) and integral cross sections (ICS) for low-energy electrons collisions HOOCl, HOClO and HClOO isomers in the range from 0.5 to 10 eV. We also present estimated dissociative electron attachment cross sections for the HClO$_2$ isomers.

Firstly, convergence and stability of the *R*-matrix calculations was investigated using procedures employed previously (Fujimoto *et al* 2012, 2014): sensitivity to the radius of the *R*-matrix sphere, *a*, was tested and also the convergence with the number of virtual orbitals (NV) included in static-exchange (SE) and static-exchange-polarisation (SEP) calculations was verified. We varied radius *a* from 10 to 15 a_0, however our results were stable and we conclude that radius with 10 a_0 was enough to get reliable results with a reasonable computation time. Therefore, the $a = 10$ a_0 was used for all isomers. The number of the virtual orbitals considered in the SEP level calculations is dependent on the basis set used to represent the molecular target. For example, when the TZV basis set is used, in the HF calculation 35 virtual orbitals are generated which can be taken to construct the $N + 1$ configurations in the equation (3); for the 6–311G* target basis set 45 virtual orbitals and for cc-pVTZ basis set 50 virtual orbitals were used, respectively. At the SE level our results can be considered converged in terms of number of the virtual orbitals for all basis sets and isomers.
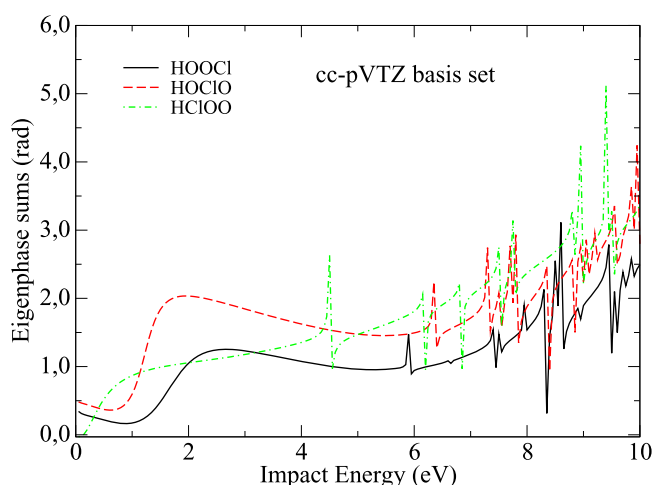
3.1. Eigenphase sums

Figure 2 presents our study of convergence of the eigenphase sum only for the most stable isomer, HOOCl, for the largest basis set cc-pVTZ where up to 50 virtual orbitals were included in the SEP calculation. When only 5 virtual orbitals are included (NV = 5) our calculations are almost without polarisation and the resonance feature lies close to 5 eV; however, when more polarisation effects are included by
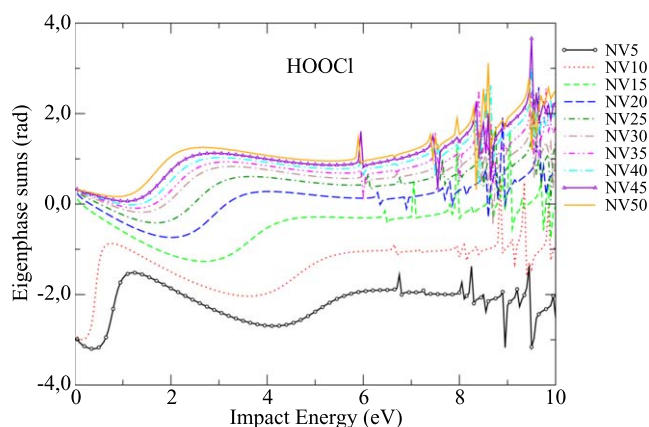
Figure 2. Convergence of the eigenphase sum for isomer HOOCl at the SEP level in terms of number of virtual orbitals (NV) for the cc-pVTZ target basis set.

Figure 3. Comparison of eigenphase sums for HOOCl, HOClO and HClOO at the SEP level for the cc-pVTZ target basis set.

increasing NV the resonance moves to lower energy and converges around 1.7 eV. Above 6 eV, many resonance structures appear; these resonances are a mixture of core-excited (Feshbach) resonances associated with excited target states and artifacts (pseudo-resonances) associated with the neglect of these states in the target expansion. Eigenphase sums for the HOOCl isomer were also computed with the other two basis sets, 6–311G* and TZV. The results are very similar, all of them find a low-energy resonance lying in the range 1.2–1.7 eV. (See the plot presented in the supplementary material as figure SG.1). All the eigenphase sums can be considered reasonable well converged for the three isomers when NV = 35 were used for TZV, NV = 45 for 6–311G* and NV = 50 for cc-pVTZ basis set. We note that calculations with NV = 5 or 10 virtual orbitals also showed a resonance structure below 1 eV; however, this structure moves below the threshold for NV ⩾ 15 giving a stable anion. It would appear that while none of the isomers have large enough permanent dipole moments to support pure dipole bound states, which would be seen at the SE level,

inclusion of polarisation effects gives one stable anion state for each isomer.

Figure 3 compares eigenphase sum for the three isomers, HOOCl, HOClO and HClOO, calculated in SEP level with cc-pVTZ basis. The second more stable isomer, HOClO, shows a low-energy resonance structure near 1.2 eV, like HOOCl. The highest energy isomer, HClOO, shows a rise in its eigenphase a very low energy which does not correspond to a full resonance; this is the only feature below 2 eV. The lowest-energy resonance for this isomer is near 4.5 eV. Automated fits of the eigenphase sums to a Breit–Wigner formula (Tennyson and Noble 1984) were used to find resonance parameters. This gave the lowest resonance positions (widths), in eV, for HOOCl, HOClO and HClOO as 1.7(1.13), 1.2(0.53) and 4.5(0.04), respectively; all resonances have ^{2}A symmetry.

Two low-lying resonances can both be seen at the static-exchange level for all three isomers which must correspond to shape resonances. Our eigenphase plots, e.g. see figure 2, show that these resonances become systematically lower in energy as NV is increased in the SEP model and that for each isomer the lowest of the two resonances becomes bound. Shape resonances can be associated with occupation of low-lying molecular orbitals so we inspected the LUMOs (lowest unoccupied molecular orbital) for each isomer. Qualitatively these do not depend on the target basis used; for each isomer the lowest LUMO is dominated by a *p* orbital localised on the Cl. For HOOCl the *p* orbital points approximately along the Cl—O bond, for HOClO it roughly points along the Cl—OH bond and for HClOO it can be thought of as being perpendicular to the approximate plane of the molecule. For HOOCl and HOClO the orbital appears to be anti-bonding while for HClOO it has a non-bonding orientation. For each isomer the second LUMO has its largest density on the H atom. For the isomers with an OH bond (HOClO and HOOCl) this accompanied by an anti-bonding arrangement along the OH bond; while for HClOO this LUMO also appears to be non-bonding. It would appear that SEP calculations stabilizes the electron in this non-bonding orbital enough that the low-lying HClOO$^-$ resonance feature being almost bound and thus giving a second HClOO$^-$ anion state.

3.2. Differential cross sections

Differential cross sections (DCSs) were computed using a number of procedures: different basis sets to represent the target molecules, SE and SEP level and with (BC) or without (WB) a Born closure procedure. Figure 4 presents DCS–BC (with Born closure) calculated at the SEP level for HOOCl using cc-pVTZ basis sets. The electron impact energy shown is 1 eV because we want to compare the polarisation effects. At this low-energy the DCS varies significantly when more polarisation effects are included (increasing NV) and with NV = 50 virtual orbitals the DCS can be considered well converged. For impact energies above 5 eV (not shown) our calculations demonstrate that the inclusion of polarisation is less significant for the DCS results. The minima observed near 45° can be attributed to the Born closure procedure as it
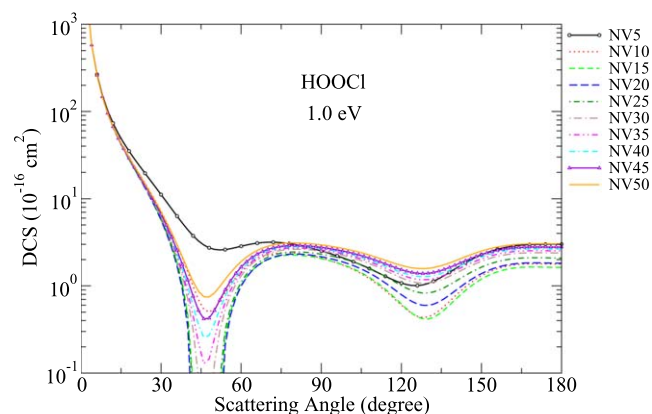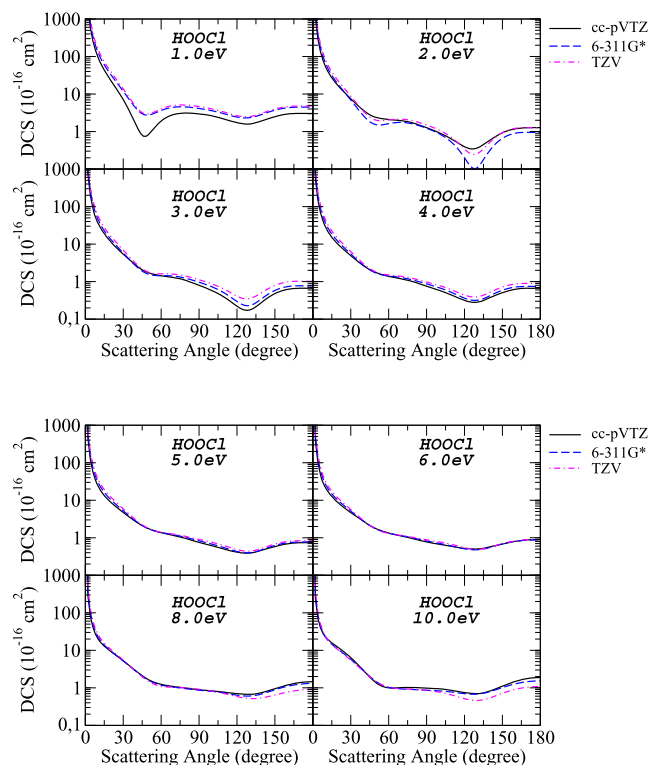
Figure 4. Dependence on polarisation of the DCS calculated at the SEP level for isomer HOOCl described using the cc-pVTZ target basis set, for an impact energy of 1.0 eV showing the dependence on the number of virtual orbitals (NV).
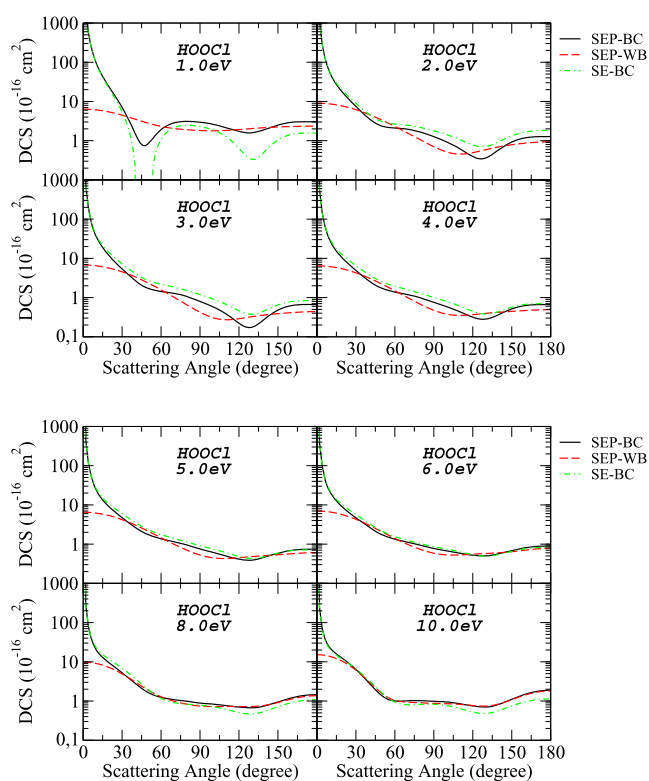
Figure 5. DCS for HOOCl described with cc-pVTZ target basis set in three different approximations: black solid line, SEP–BC, static-exchange-polarisation with Born closure procedure; red dash line, SEP–WB, static-exchange-polarisation with no Born closure; dashed–dotted green line SE–BC static-exchange with Born closure procedure. For impact energies 1, 2, 3, 4, 5, 6, 8 and 10 eV.

is not observed in our DCS–WB (without Born closure) calculations where the dipole long-range interaction are not fully included. Presumably this is caused by a cancellation between the effects of the target dipole and the polarisation potential, as evidenced by the fact that the minimum essentially disappears when NV = 5.

The influence of Born closure and polarisation effects can be found by comparing DCS–SEP–BC, DCS–SEP–WB and DCS–SE–BC results which are plotted in figure 5. The

Figure 6. Basis sets dependence of the DCS calculated in SEP–BC level for isomer HOOCl calculated with three basis sets: TZV, 6–311G* and cc-pVTZ. For impact energies 1, 2, 3, 4, 5, 6, 8 and 10 eV.

comparison between DCS–SEP–BC, DCS–SE–BC shows that polarisation effects are more important for impact energies below 5 eV, since both calculations take into account dipole long-range interaction with Born closure. Although SEP–BC and SE–BC present very good qualitative agreement even for lower energies where the long-range dipole effects dominate. The comparison between the SEP–BC and SEP–WB results confirms the importance of taking into account partial waves beyond $\ell_{max} = 4$ as all of three isomers have permanent dipole moment. At lower energies there are also qualitative difference between SEP–BC and SEP–WB calculations. The DCS–SEP–WB has a minimum around 90° indicating significant contributions of p partial waves while DCS–SEP–BC the minima are at 45° and 135° seem to suggest a predominance of d partial waves. In general, for higher scattering energies there is quantitative agreement for angles greater than 30°. The divergent behaviour in DCS–SEP–BC at very low angles is expected due to long-range interactions when higher partial waves are included due to permanent dipole moment, and is known to make an important contribution to the integral cross section (ICS) (Zhang *et al* 2009).
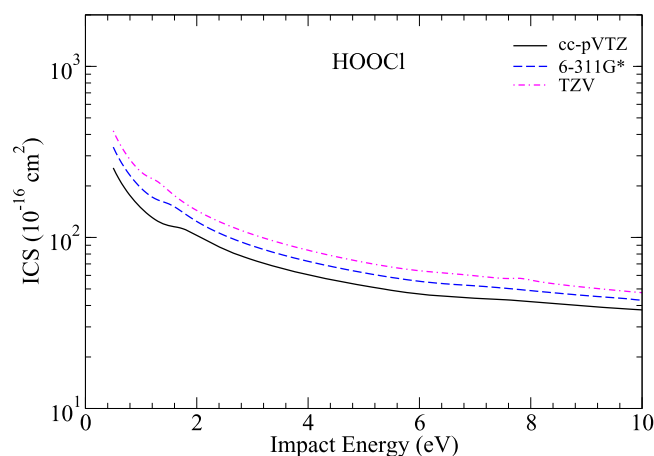
Figure 6 explores the dependence of the DCS on the three target basis sets used to describe HOOCl. The DCS are calculated in SEP–BC level and the molecular orbitals are represented by the basis sets: TZV, 6–311G* and cc-pVTZ. At lower scattering energies of 1–3 eV, the differences in the DCS can be mainly attributed to the description of scattering

J. Phys. B: At. Mol. Opt. Phys. **52** (2019) 165201

M M Fujimoto *et al*
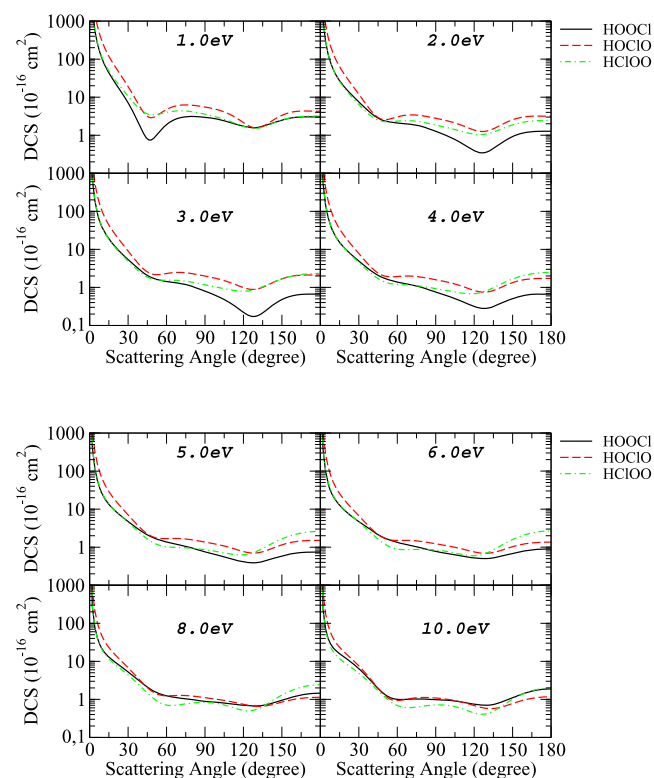
Figure 7. Comparison of DCS calculated at the SEP–BC level for the HOOCl, HOClO and HClOO isomers calculated using cc-pVTZ basis set. For impact energies 1, 2, 3, 4, 5, 6, 8 and 10 eV.

Figure 8. Integral cross section (ICS) for HOOCl calculated with SEP plus Born closure. Dependence of ICS on three different target basis sets: TZV, 6–311G* and cc-pVTZ.

potential which varies as a function of the basis set chosen to represent the target; this affects slow electrons more than fast electrons. The reason is that as the size of basis sets differ, they yield different polarisation effects. This can be seen in figure 3 where the low-energy resonance feature is not precisely in the same position although the calculation is converged for each basis set. The small differences in the resonance position is the main cause of difference in the DCS at energies below 3 eV. At higher energies, the 6–311G* and cc-pVTZ results are closer to each other than the DCS–TZV results, indicating a convergence in DCS results for the larger basis sets.

Figure 7 compares the DCS–SEP–BC for the three isomers, HOOCl, HOClO and HClOO calculated with cc-pVTZ basis sets for impact energies of 1–10 eV. At angles below 30°, the DCS of HOOCl and HClOO converge; this forward scattering is dominated by the long-range interactions due to the dipole moment which is taken into account by Born closure and the permanent dipole moments for these isomers are both about 1.9 Debye. The DCS for HOClO shows a more pronounced increase in the forward direction due to its larger dipole of 3.2 Debye. All isomers show a similar structure in the DCS with minima near 45° and 135° indicating the preponderance of *d*-partial waves. At lower impact energies, below 4 eV, the DCS of HOClO and HClOO are very close for angles higher than 30°; this can be attributed to the similarity of the two molecular structure, both have an O–Cl–O backbone and they only differ in the position of the H atom. At higher energies, above 5 eV, the DCS of HOOCl and HOClO

become more similar at angles higher than 30°, probably because the similarity of the shape of molecules: both are elongated compared to HClOO, giving similar electronic densities.

3.3. Integral cross sections

Figure 8 shows our comparative study of the influence of basis set choice in the ICS–SEP calculated with Born closure technique for the HOOCl isomer. The TZV is the smaller basis set but gives a larger permanent dipole and a larger ICS at all impact energies compared to the other basis sets. The difference in ICS reduces as the energy increases. If we also compare with our results of ICS–SEP without Born closure (not shown) we conclude that the permanent dipole moment further scales the cross section when a Born closure procedure is used. The same behaviour was observed by us for different conformers of alanine (Fujimoto *et al* 2016) and beta-alanine (Fujimoto *et al* 2017). Table 1 gives the value of the dipole moment for each the basis set used; we observe that the magnitude order of the ICS follows that of the dipole moment. If we take the largest basis set, cc-pVTZ, as our reference, the ICS calculated shows that the basis set choice are less important when the impact energies increases, which is expected. The difference between ICS at 5 eV are around 45% for TZV and 22% for 6–311G*, indicating the ICS results are converging to a given results with the increase of the basis set. At 10 eV, these differences reduce to 15% for TZV and 7% for 6–311G*. Above 6 eV some irregular oscillations in the ICS could be attributed to the large number of $N + 1$ configurations generated in the SEP calculations as expressed in equation (3). These oscillations are associated with the large number of the resonances, either core-excited or pseudo, in the SEP calculations.

Figure 9 compares the ICS calculated at the SEP level using the cc-pVTZ basis and including Born correction for the three isomers, HOOCl, HOClO and HClOO. The HOClO, the second lowest energy isomer, show bigger ICS at all the impact energy range considered. The reason for this, which
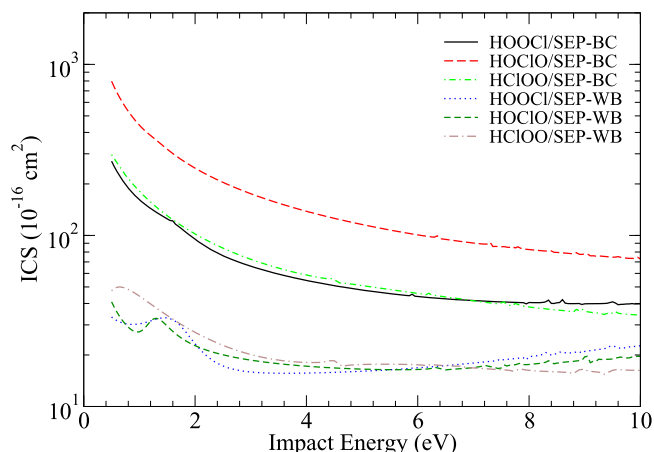
Figure 9. Comparison of the integral cross section (ICS) calculated at the SEP level with the cc-pVTZ target basis and including (BC) or not (WB) the Born correction for the three isomers: HOOCl, HOClO and HClOO.

also explains the similarity in the ICS between HOOCl and HClOO, is that the ICS scales approximated with the square permanent dipole moment. Comparing our results with (BC) and without Born (WB) correction, the resonance feature observed in ICS–WB for HOOCl and HOClO are practically washed out in the results including Born corrections (ICS–BC).

3.4. DEA cross sections

Dissociative electron attachment (DEA) is a process that occurs when a low-energy electron is captured by a molecule, generally forming a temporary anion which decays into fragments. This process can be a path to release species in the atmosphere by fragmentation of $HClO_2$ isomers. In a simple way DEA could be represented by

$$AB + e^- \rightarrow (AB^-)^* \rightarrow A^- + B \text{ or } A + B^-, \quad (4)$$
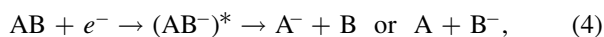
where A and B are the neutral fragments, and A^- and B^- are the charged species (anions); $(AB^-)^*$ is the temporary molecular anion or resonance.

In this section, we present our evaluation of DEA cross sections to interactions of low-energy electrons (<5 eV) with $HClO_2$ isomers which were calculated based on the DEA estimator procedure of Munro *et al* (2012). In this procedure the estimated DEA cross sections, $\sigma(E)$, is given by:

$$\sigma(E) = C \sum_{i=1} S_i \sigma_{ri}(E), \quad (5)$$

where S_i is the survival probability of the temporary anion, $\sigma_{ri}(E)$ is the resonant cross section associated with the *i*th resonance; C is an empirically-determined coefficient which is used to allow for the physics not taken into account by the simple model. Here, instead of estimating the classical time by equation (10) of Munro *et al* (2012), we use $t = \int_{r_e}^{r_c} \frac{1}{v(r)} dr$, where $v(r)$ is the velocity of the reduced mass particle of fragments as a function of position when it is moving from r_e to r_c in the potential energy curve, r_e is the equilibrium distance and r_c is the crossing point between resonance potential

Table 3. Spectroscopic parameters used in DEA estimator model to calculated DEA cross sections of HOOCl, HOClO and HClOO isomers.

Process	r_e[a]	D_e[b]	E_a	ν[c]
Isomer HOOCl				
$HOO–Cl^- \rightarrow HOO + Cl^-$	r_e(O–Cl) 1.723	1.723	3.613[d]	361
$HOO–Cl^- \rightarrow HOO^- + Cl$	1.723 12		1.089[e]	
Isomer HOClO				
$HO–OCl^- \rightarrow OH + ClO^-$	r_e(O–O) 1.236	1.236	2.276[f]	835
$HO–OCl^- \rightarrow OH^- + ClO$	1.424 90		1.827[g]	
$HO–ClO^- \rightarrow OH + ClO^-$	r_e(O–Cl) 0.850	0.850	2.276[f]	540
$HO–ClO^- \rightarrow OH^- + ClO$	1.715 43		1.827[g]	
Isomer HClOO				
$H–ClOO^- \rightarrow H + ClOO^-$	r_e(H–Cl) 1.990	1.990	3.660[h]	2168
$H–ClOO^- \rightarrow H^- + ClOO$	1.347 24		0.754[i]	
$HClO–O^- \rightarrow HClO + O^-$	r_e(Cl–O) 3.500[k]	3.500[k]	1.461[j]	1093
$HClO–O^- \rightarrow HClO^- + O$	1.485 52		3.640[k]	

[a] r_e equilibrium distance between named two atoms in Å.
[b] D_e bond dissociation energy in eV from Sumathi and Peyerimhoff (1999), unless specified.
[c] ν vibrational frequencies in cm^{-1} from Francisco *et al* (1994). Electron Affinities (E_a) in eV.
[d] From Berzinsh *et al* (1995).
[e] From Clifford *et al* (1998).
[f] From Gilles *et al* (1992).
[g] From Smith *et al* (1997).
[h] From Distelrath and Boesl (2000).
[i] From Lykke *et al* (1991).
[j] From Blondel (1995).
[k] Values estimated from CASSCF calculations performed using Molpro (Werner *et al* 2012).

and the Morse potential of neutral target. To allow for this change we re-calibrated C to minimises the difference in the DEA cross sections for Cl_2 (Kurepa and Belic 1978) and O_2 (Rapp and Briglia 1965) which gave $C = 0.1334$. For all the three isomers it was considered only the lowest-energy resonance which leads to break up the molecule. Basically we allow straight breaking of the chemical bond, the mechanism of atomic rearrangement is not considered explicitly. In DEA estimator computational program beyond of resonance position and width to calculate DEA cross sections, the model needs data related to the specific chemical bond which will break up, such as: equilibrium distance (r_e), dissociation energy (D_e); vibrational frequency (ν) and the electron affinity (E_a) of the produced anion. The important data used in the model to estimate the DEA cross sections are given in the table 3. All vibrational frequencies were taken from Francisco *et al* (1994); dissociation energies for the isomers were taken from the Sumathi and Peyerimhoff (1999) unless indicated. For electron affinities there is a good review in Rienstra-Kiracofe *et al* (2002) and references therein. Only exception is for E_a and D_e for $HClO^-$ which were estimated by a complete active space self-consistent field (CASSCF)
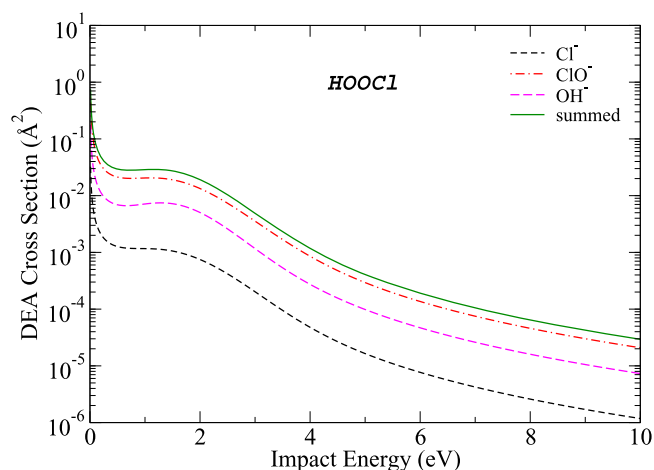
Figure 10. DEA Cross sections for HOOCl in function of impact energy. Considering following reactions: HOO–Cl$^-$ → HOO + Cl$^-$ and HO–OCl$^-$ → OH + ClO$^-$ or OH$^-$ + ClO.

Figure 11. DEA Cross sections for HOClO in function of impact energy. Considering following reactions: HO–ClO$^-$ → OH + ClO$^-$ or OH$^-$ + ClO.

(Roos *et al* 1980) calculation using Molpro (Werner *et al* 2012). A hyphen, '-', in the chemical formula of anion is used to show where the bond is being broken.

3.4.1. HOOCl DEA cross sections. For HOOCl, the very broad, low-energy resonance located at 1.70 eV can lead to the two bond breaks generating three charged species and their neutral counterparts:
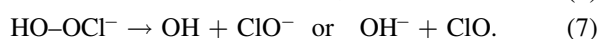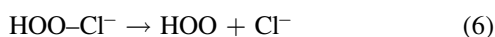
$$HOO–Cl^- → HOO + Cl^- \qquad (6)$$

$$HO–OCl^- → OH + ClO^- \quad or \quad OH^- + ClO. \qquad (7)$$

Figure 10 presents the DEA cross sections for HOOCl considering only one resonant state formed at 1.7 eV which decay into fragments. According to this estimate three processes generate charged species. The process that generates ClO$^-$ has the largest DEA cross sections in all range of energies, followed by OH$^-$ and the Cl$^-$ is the smallest. The neutral OH, ClO and HOO are also expected to be produced and some of these species are known to be important in the catalytic destruction of ozone. The production of Cl radical by straight breaking of HOOCl is a process of very low efficiency, the magnitude of cross section is near 10^{-9} Å^2, probably because the electron affinity of HOO$^-$ is relatively small. We do not observe breaking of H–O bond to the HOOCl molecule, because the resonance potential do not cross with the neutral target potential curve in our calculation. Maybe it could be properly estimated if accurate Morse potentials for resonant and neutral species are available. The DEA cross section is estimated to be 0.026 Å^2 at 1.7 eV. Figure 10 also shows the partial DEA cross sections for the processes that generate ClO$^-$, OH$^-$ and Cl$^-$ which contribute around 71%, 25% and 4% of the total cross section, respectively.

3.4.2. HOClO DEA cross sections. The HOClO molecule has a broad, low-energy resonance at 1.2 eV that decays into charged fragments of ClO$^-$ and OH$^-$ and corresponding neutral radicals. Figure 11 shows that the DEA cross sections
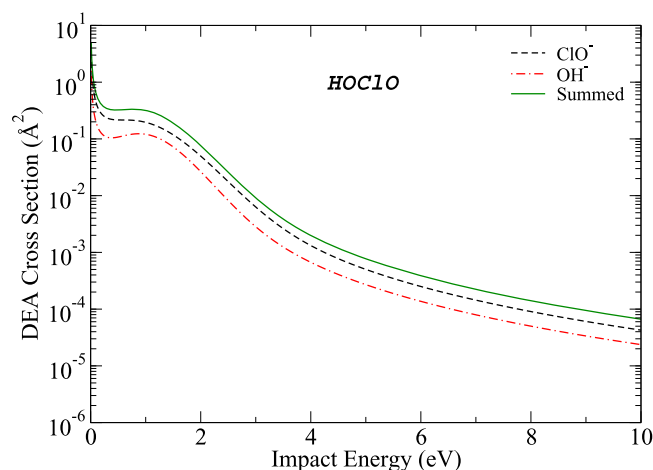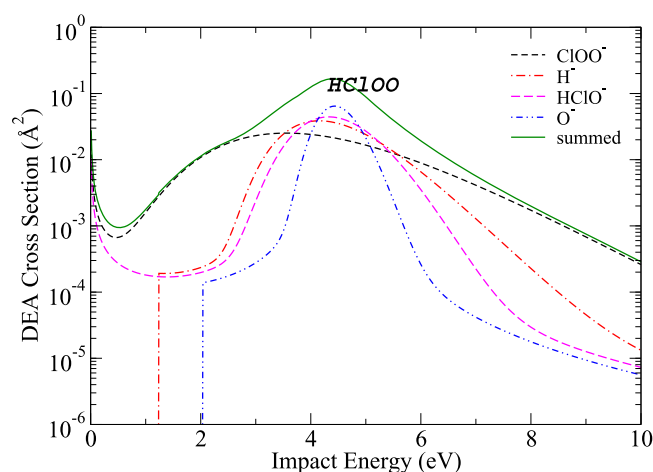
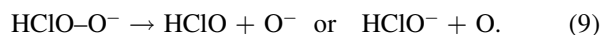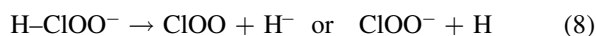

Figure 12. DEA Cross sections for HClOO in function of impact energy. Considering following reactions: H–ClOO$^-$ → H + ClOO$^-$ or H$^-$ + ClOO and HClO–O$^-$ → HClO + O$^-$ or HClO$^-$ + O.

for the processes that generate ClO$^-$ have higher probability than OH$^-$ in all range of energies. The only possibility considered of breaking was the O–Cl bond of HO–ClO$^-$ anion. For the other bonds, H–O and Cl–O, the DEA cross sections was not calculated because the electron affinity estimated for HOC$^-$ give negative value and also our resonance potential do not cross the Morse potential of the neutral target. For this isomer, the summed DEA cross sections give 0.28 Å^2 at 1.2 eV, an order of magnitude higher than HOOCl at its resonance energy. However, DEA of HOOCl leads to greater variety of anion and neutral species than HOClO.

3.4.3. HClOO DEA cross sections. The HClOO isomer do not have a resonance below 2 eV, so we do not expect significant DEA cross sections in this energy range. In general, DEA is less important at higher electron collision energies where other processes can also lead to the

J. Phys. B: At. Mol. Opt. Phys. **52** (2019) 165201

M M Fujimoto *et al*

destruction of molecules so we expect that the DEA process may not be important for this isomer. The lowest-energy HClOO resonance is a narrow one at 4.5 eV. We estimate the DEA cross sections to verify the behaviour of HClOO at lower energies. Figure 12 shows DEA cross sections for HClOO; the following four processes are considered:

$$H–ClOO^- \rightarrow ClOO + H^- \quad \text{or} \quad ClOO^- + H \quad (8)$$

$$HClO–O^- \rightarrow HClO + O^- \quad \text{or} \quad HClO^- + O. \quad (9)$$

The dissociation pathways which produce HCl and O_2 are not considered because they involve rearrangement of atoms. The summed DEA cross sections near 1.7 eV is only $7 \times 10^{-3} \text{ Å}^2$ and the maximum near 4.4 eV is around 0.17 Å^2. Near their resonance energies, the HClOO isomer has DEA cross sections smaller than HOClO, however present larger cross section than HOOCl, probably due to the higher relative stability of HOOCl which is the most stable isomer.

4. Conclusions

This work presents a first study of the electron-scattering cross sections of the isomers HOOCl, HOClO and HClOO. The UK molecular *R*-matrix codes is employed and we perform test of *R*-matrix radius, atomic basis sets (TZV, 6–311G* and cc-pVTZ), number of virtual orbital (SE and SEP levels) and Born closure procedure. The cross sections can be considered reasonably well converged with respect to the number of virtual orbitals used in SE and SEP calculations for all basis sets tested. The eigenphase sums have show that HOOCl and HOClO isomers possess resonance below 2 eV and the lowest energy resonance for HClOO is near 4.5 eV in a SEP level calculation. Figure 6 shows the importance of the atomic basis set in describing the target at impact energies below 5 eV. At higher energies the DCS are less dependent of the choice of basis set. The three isomers show DCSs of similar magnitude and qualitative behaviour; differences between them diminish going to higher scattering energies. Choice of target basis set is more important at lower energies for both the DCS and the ICS. Particular case is required if the target has a permanent dipole as at low-energy the ICS depends approximately on the dipole squared. It is therefore necessary to test dependence of the permanent dipole moment on the basis sets to get reliable ICS. Estimated DEA cross sections for $HClO_2$ isomers are presented for the first time and indicate that HOOCl and HOClO can fragment via DEA with low-energy electrons while significant DEA for HClOO is only expected at somewhat higher energies.

Acknowledgments

ORCID iDs

Jonathan Tennyson https://orcid.org/0000-0002-4994-5238

References

Barrett J W, Solomon P M, de Zafra R L, Jaramillo M, Emmons L and Parrish A 1988 *Nature* **336** 455–8

Berzinsh U, Gustafsson M, Hanstorp D, Klinkmüller A, Ljungblad U and Mårtensson-Pendrill A-M 1995 *Phys. Rev. A* **51** 231–8

Blondel C 1995 *Phys. Scr.* **T58** 31–42

Bode M and Gordon M S 1998 *J. Mol. Graph. Model.* **16** 133–8

Boudaïffa B, Cloutier P, Hunting D, Huels M A and Sanche L 2000 *Science* **287** 1658–60

Carr J M, Galiatsatos P G, Gorfinkiel J D, Harvey A G, Lysaght M A, Madden D, Mašín Z, Plummer M, Tennyson J and Varambhia H N 2012 *Eur. Phys. J. D* **66** 58

Cattell F C and Cox R A 1986 *J. Chem. Soc., Faraday Trans. 2* **82** 1413–26

Christophorou L G and Stockdale J A D 1968 *J. Chem. Phys.* **48** 1956–60

Clifford E P, Wenthold P G, Gareyev R, Lineberger W C, DePuy C H, Bierbaum V M and Ellison G B 1998 *J. Chem. Phys.* **109** 10293–310

Colussi A J and Grela M A 1993 *J. Phys. Chem.* **97** 3775–9

Cox R A 2003 *Chem. Rev.* **103** 4533–48

de Souza G L C and Brown A 2017 private communication

Distelrath V and Boesl U 2000 *Faraday Discuss.* **115** 161–74

Dubey M K, McGrath M P, Smith G P and Rowland F S 1998 *J. Phys. Chem. A* **102** 3127–33

Dunning T H Jr 1971 *J. Chem. Phys.* **55** 716–23

Dunning T H Jr 1989 *J. Chem. Phys.* **90** 1007–23

Farman J C, Gardiner B G and Shanklin J D 1985 *Nature* **315** 207–10

Faure A, Gorfinkiel J D, Morgan L A and Tennyson J 2002 *Comput. Phys. Commun.* **144** 224–41

Feller D 1996 *J. Comp. Chem.* **17** 1571–86

Francisco J S, Sander S P, Lee T J and Rendell A P 1994 *J. Phys. Chem.* **98** 5644–9

Fujimoto M M, Brigg W J and Tennyson J 2012 *Eur. J. Phys. D* **66** 204

Fujimoto M M, de Lima E V R and Tennyson J 2016 *J. Phys. B: At. Mol. Opt. Phys.* **49** 215201

Fujimoto M M, de Lima E V R and Tennyson J 2017 *J. Phys. B: At. Mol. Opt. Phys.* **50** 195201

Fujimoto M M, Tennyson J and Michelin S E 2014 *Eur. Phys. J. D* **68** 67

Gillan C J, Tennyson J and Burke P G 1995 *Computational Methods for Electron-Molecule Collisions* ed F A Gianturco (New York: Plenum) pp 239–54

Gilles M K, Polak M L and Lineberger W C 1992 *J. Chem. Phys.* **96** 8012–20

Johnsson K, Engdahl A and Nelander B 1996 *J. Phys. Chem.* **100** 3923–6

Krishnan R, Binkley J S, Seeger R and Pople J A 1980 *J. Chem. Phys.* **72** 650–4

J. Phys. B: At. Mol. Opt. Phys. **52** (2019) 165201

M M Fujimoto *et al*

Kurepa M V and Belic D S 1978 *J. Phys. B: At. Mol. Phys.* **11** 3719–29

Lee T J and Rendell A P 1993 *J. Phys. Chem.* **97** 6999–7002

Lee Y-P and Howard C J 1982 *J. Chem. Phys.* **77** 756–63

Lykke K R, Murray K K and Lineberger W C 1991 *Phys. Rev.* A **43** 6104–7

McGrath M P, Clemitshaw K C, Rowland F S and Hehre W J 1990 *J. Phys. Chem.* **94** 6126–32

McLean A D and Chandler G S 1980 *J. Chem. Phys.* **72** 5639–48

Molina L T and Molina M J 1987 *J. Phys. Chem.* **91** 433–6

Molina M J and Rowland F S 1974 *Nature* **249** 810–2

Morrison M A 1988 *Adv. At. Mol. Phys.* **24** 51–156

Munro J J, Harrison S, Fujimoto M M and Tennyson J 2012 *J. Phys.: Conf. Ser.* **388** 012013

National Research Council 1989 *Ozone Depletion, Greenhouse Gases, and Climate Changes* (Washington, DC: The National Academies Press) pp 1–102

Padial N T, Norcross D W and Collins L A 1981 *J. Phys. B: At. Mol. Phys.* **14** 2901–9

Phillips D H and Quelch G E 1996 *J. Phys. Chem.* **100** 11270–5

Rapp D and Briglia D D 1965 *J. Chem. Phys.* **43** 1480–9

Rienstra-Kiracofe J C, Tschumper G S, Schaefer H F III, Nandi S and Ellison G B 2002 *Chem Rev* **102** 231-282

Roos B O, Taylor P R and Siegbahn P E M 1980 *Chem. Phys.* **48** 157–73

Sanna N and Gianturco F A 1998 *Comput. Phys. Commun.* **114** 142–67

Schuchardt K L, Didier B T, Elsethagen T, Sun L, Gurumoorthi V, Chase J, Li J and Windus T L 2007 *J. Chem. Inf. Model.* **47** 1045–52

Smith I W M 2003 *Chem. Rev.* **103** 4549–64

Smith J R, Kim J B and Lineberger W C 1997 *Phys. Rev.* A **55** 2036–43

Sumathi R and Peyerimhoff S D 1999 *J. Phys. Chem.* A **103** 7515–21

Tennyson J 1996 *J. Phys. B: At. Mol. Opt. Phys.* **29** 1817–28

Tennyson J 2010 *Phys. Rep.* **491** 29–76

Tennyson J and Noble C J 1984 *Comput. Phys. Commun.* **33** 421–4

Turner A G and Oleksik J 1991 *Inorg. Chim. Acta* **180** 15–7

Watchers A J H 1970 *J. Chem. Phys.* **52** 1033–6

Weissman M, Shum L G S, Heneghan S P and Benson S W 1981 *J. Phys. Chem.* A **85** 2863–6

Werner H-J, Knowles P J, Knizia G, Manby F R and Schütz M 2012 *WIREs Comput. Mol. Sci.* **2** 242–53

Yoshinobu T, Akai N, Kawai A and Shibuya K 2009 *Chem. Phys. Lett.* **477** 70–4

Zhang R, Faure A and Tennyson J 2009 *Phys. Scr.* **80** 015301

Zhu R S, Xu Z F and Lin M C 2002 *J. Chem. Phys.* **116** 7452–60